Electronic Supplementary Material (ESI) for Analyst.

Supporting Information

An electrochemical biosensor for T4 polynucleotide kinase activity assay according to host-guest recognition among phosphate pillar[5]arene@MWCNTs and thionine

Aiwen Su,[a] Dan Luo,[a] Shixuan Li,[a] Yanli Zhang,*[a] Hongbin Wang,[a] Lijuan Yang,*[a] Wenrong Yang[a] and Pengfei Pang*[a]

[a] *Key Laboratory of Environmental Functional Materials of Yunnan Province Education Department, Yunnan Minzu University, Kunming 650504, P. R. China. E-mail*: ylzhang@ymu.edu.cn, yangljyang@sina.com, pfpang@aliyun.com

[b] *School of Life and Environmental Sciences, Deakin University, Geelong, VIC 3217, Australia*

Supporting figure captions:

Scheme S1 Synthetic route for phosphate pillar[5]arenes (PP5).

Fig. S1 SEM image of prepared PP5. Inset is the high resolution SEM image of PP5.

Fig. S2 EDS spectrum of PP5@MWCNTs.

Fig. S3 Zeta potential of (A) MWCNTs and (B) PP5@MWCNTs.

Fig. S4 (A) UV-vis absorption spectra and (B) fluorescent emission spectra of thionine with different concentration of PP5.

Fig. S5 Optimization of experimental parameters. The effects of concentration of ATP (A), phosphorylation time (B), concentration of TiO_2 (C) and Thi (D), and incubation time (E) on T4 PNK activity assay. The assays were carried out in 100 mM PBS (pH 7.4) containing 15 U mL^{-1} T4 PNK.

Fig. S6 The inhibition effects of (A) $(NH_4)_2SO_4$, (B) ADP, and (C) EDTA on T4 PNK activity. The concentration of T4 PNK is 15 U mL^{-1}.

Fig. S7 DPV response curves of biosensor *vs.* spiked different concentrations of T4 PNK (0.001, 0.01, 0.1, 1, 5 U mL^{-1}) in 100 mM PBS (pH 7.4).

Table S1

Comparison of the analytical performances of proposed electrochemical biosensor for T4 PNK activity assay with other reported methods

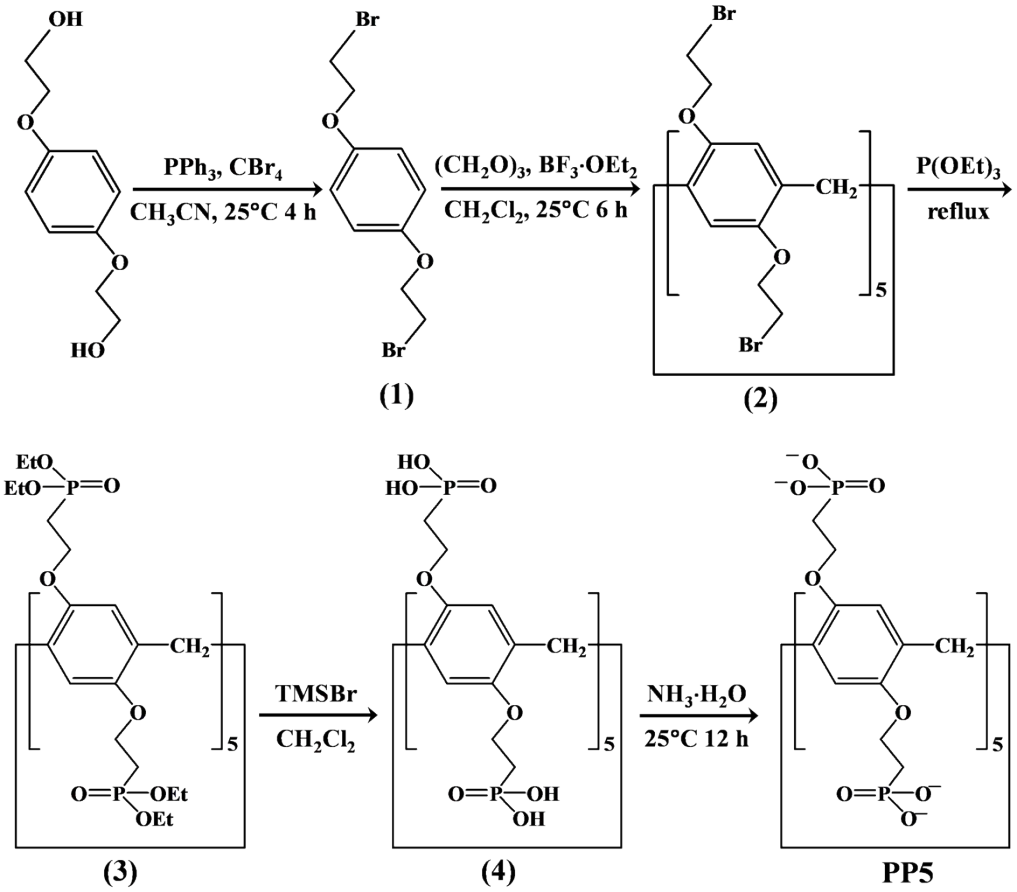

Scheme S1 Synthetic route for phosphate pillar[5]arenes (PP5).

PP5 synthesis

Synthesis route of PP5 was illustrated in Scheme S1, including five processes. (1) At 0 ℃, while stirring, 1,4-bis(2-hydroxyethoxy)benzene (10 g) and triphenylphosphine (PPh3, 32 g) were added to 200 mL of acetonitrile (CH_3CN). Carbon tetrabromide (CBr_4, 40 g) was added, and solution agitation had been approached at 25 ℃ for 4 hours with N_2. The reaction was stopped by adding 200 mL of cold water, at which point product 1 crystallized out as a white solid. Filtration was used to harvest product 1, which was then alternatively washed in ethanol and deionized water before being dried in a vacuum. Stirring 4 g of product 1 and 1.1 g of trioxymethylene ($(CH_2O)_3$) in 200 mL of dichloromethane (CH_2Cl_2) produced a clear solution. After adding 1.8 g of boron trifluoride etherate (BF_3OEt_2) to the mixture, it was agitated for 6 hours at 25 ℃. After adding deionized water (10 mL) to halt the reaction, mixture washing and drying over Na_2SO_4 could be done. Product 2 was obtained as a white

solid after solvent evaporation, with additional refining using petroleum ether/CH_2Cl_2 (1:1, v/v) based column chromatography. (3) At 165 ℃, under N_2, product 2 (2.5 g) was combined with triethyl phosphite ($P(OEt)_3$, 10 g) and agitated for 3 days. After that, silica gel chromatography was performed on the crude product using methanol and the eluent ethyl acetate (1:2, v/v). Additionally, product 3 was successfully obtained as a pale yellow oil. (4) In 40 mL CH_2Cl_2 at 0 ℃ under N_2, product 3 (3 g) and trimethylsilyl bromide (TMSBr) (14 g) were added. For three days, 25 ℃ was utilized for agitating the reaction mixture. The solvent was evaporated at low pressure, and the remaining yellow oily liquid was mixed with 30 mL of deionized water over the course of 30 minutes. After low pressure solvent evaporation, a light yellow solid could be produced as the crude product. After being washed with acetone, the desired product 4, a white solid, was obtained. (5) At 25 ℃, 100 mL of $NH_3 \cdot H_2O$ was mixed with 0.2 g of product 4. This mixture was agitated for 12 hours. Under decreased pressure, the solvent was absorbed, leaving a light-yellow clear solid that was identified as PP5.

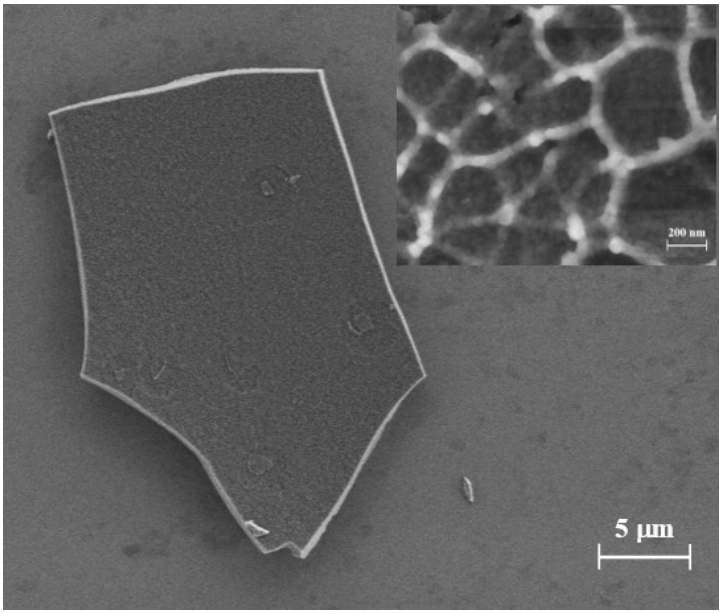

Fig. S1 SEM image of prepared PP5. Inset is the high-resolution SEM image of PP5.

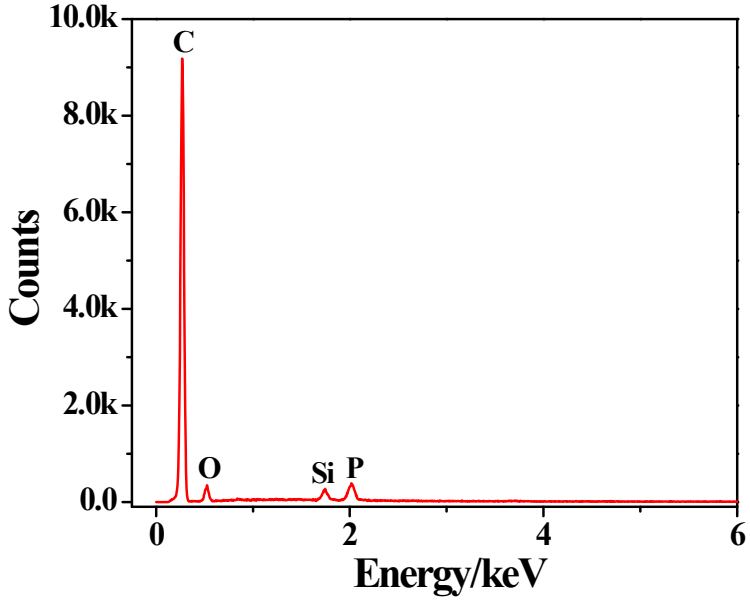

Fig. S2 EDS spectrum of PP5@MWCNTs.

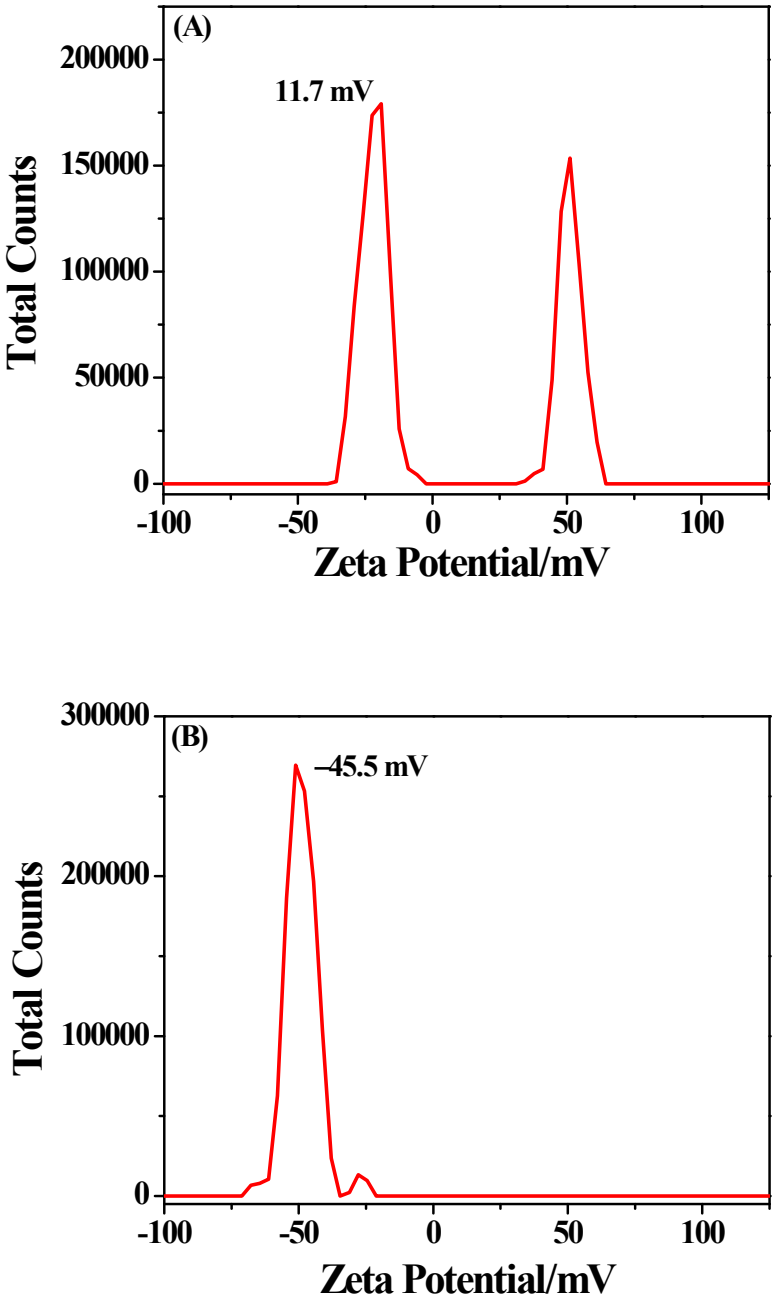

Fig. S3 Zeta potential of (A) MWCNTs and (B) PP5@MWCNTs.

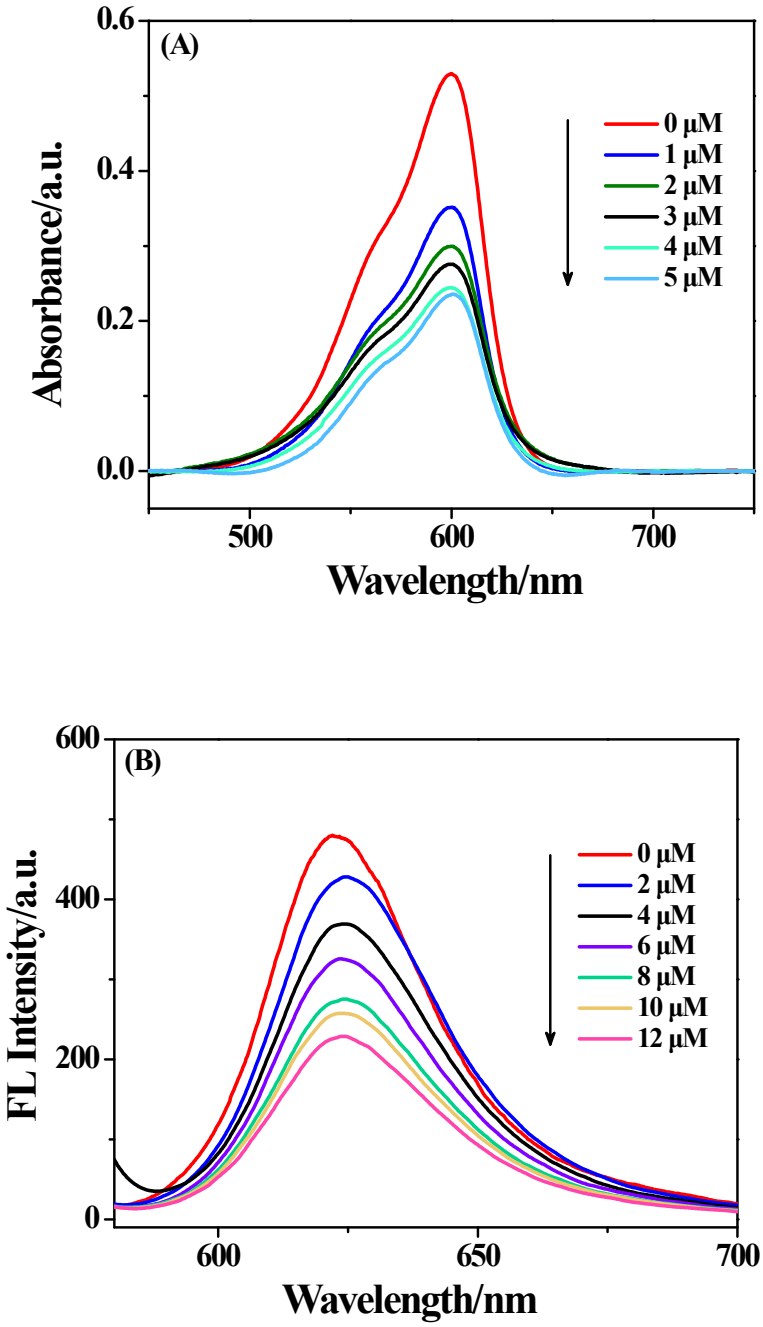

Fig. S4 (A) UV-vis absorption spectra and (B) fluorescent emission spectra of thionine with different concentration of PP5.

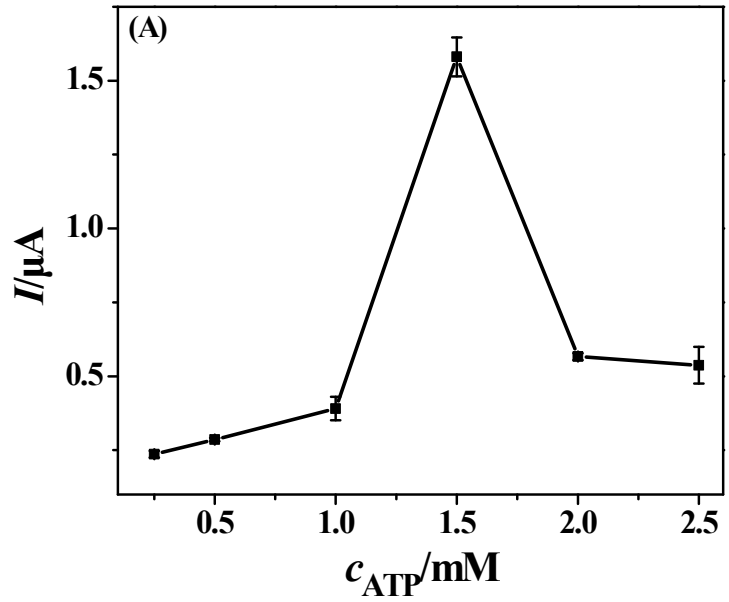
(A)
1.5
1.0
0.5
I/μA
0.5
1.0
1.5
2.0
2.5
c_ATP/mM

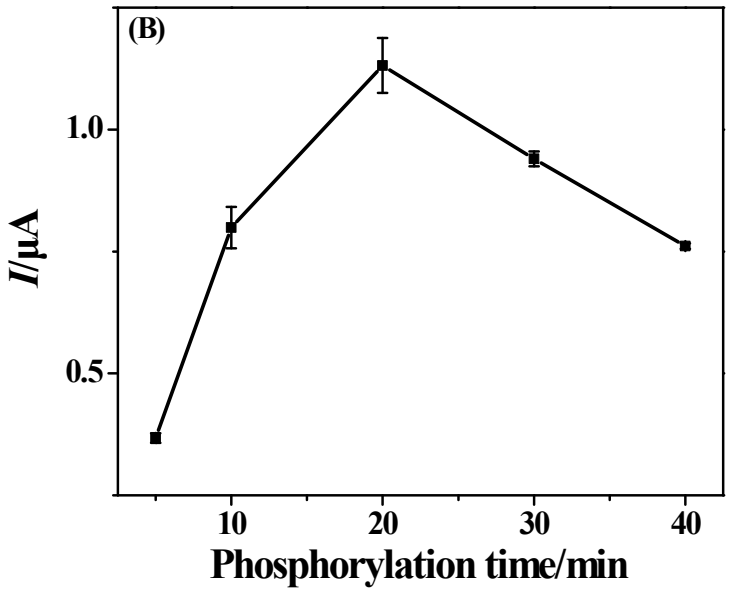
(B)
1.0
0.5
I/μA
10
20
30
40
Phosphorylation time/min

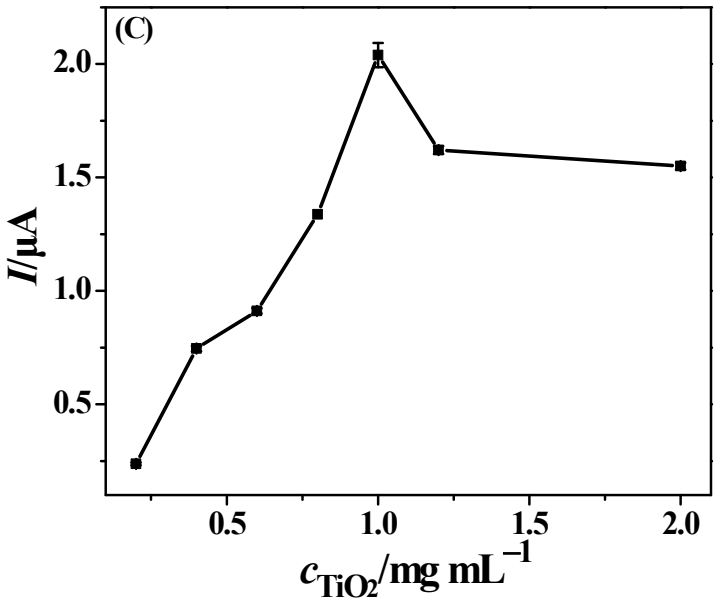
(C)
2.0
1.5
1.0
0.5
I/μA
0.5
1.0
1.5
2.0
c_{TiO2}/mg mL^{-1}

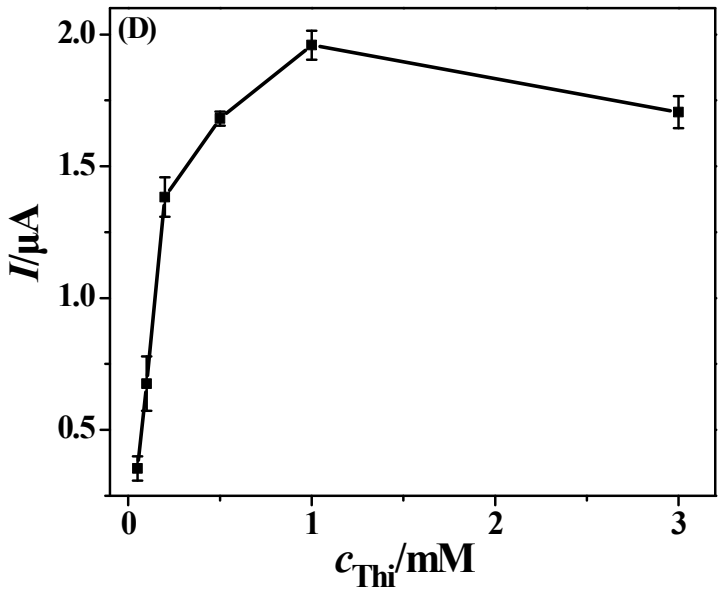
(D)
2.0
1.5
1.0
0.5
I/μA
0
1
2
3
c_{Thi}/mM

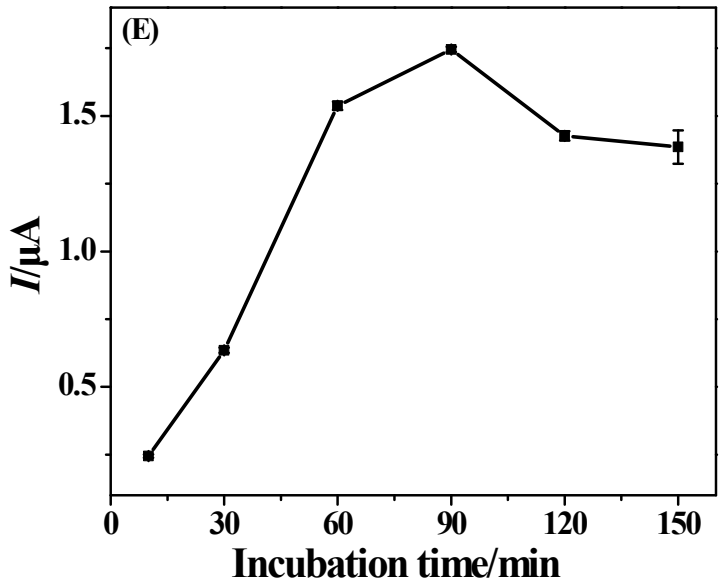

Fig. S5 Optimization of experimental parameters. The effects of concentration of ATP (A), phosphorylation time (B), concentration of TiO_2 (C) and Thi (D), and incubation time (E) on T4 PNK activity assay. The assays were carried out in 100 mM PBS (pH 7.4) containing 15 U mL^{-1} T4 PNK.

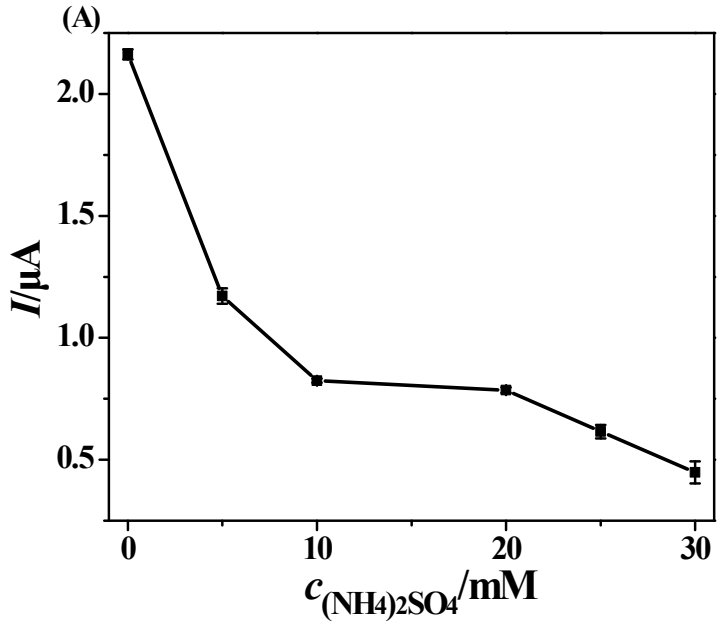
(A)
2.0
1.5
1.0
0.5
I/μA
0
10
20
30
c(NH4)2SO4/mM

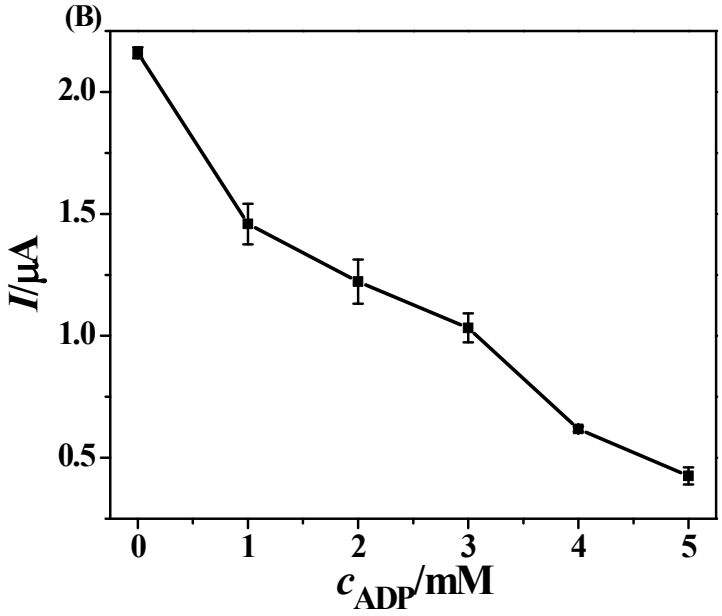
(B)
2.0
1.5
1.0
0.5
I/μA
0
1
2
3
4
5
cADP/mM

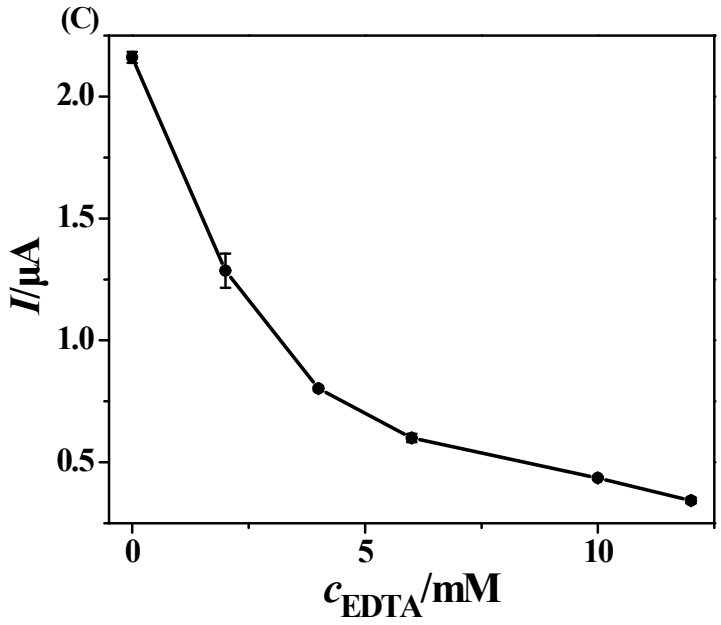

Fig. S6 The inhibition effects of (A) $(NH_4)_2SO_4$, (B) ADP, and (C) EDTA on T4 PNK activity. The concentration of T4 PNK is 15 U mL^{-1}.

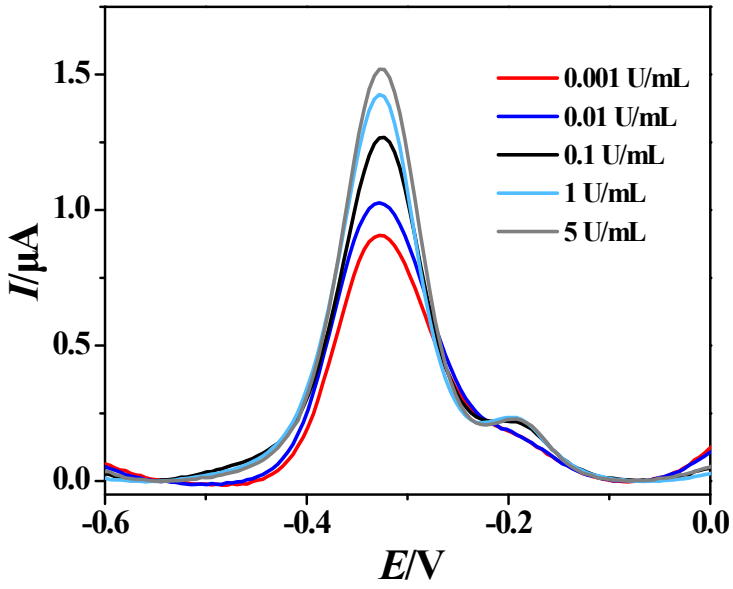

Fig. S7 DPV response curves of biosensor *vs.* spiked different concentrations of T4 PNK (0.001, 0.01, 0.1, 1, 5 U mL^{-1}) in 100 mM PBS (pH 7.4).

Table S1

Comparison of the analytical performances of proposed electrochemical biosensor for T4 PNK activity assay with other reported methods

Strategy	Technique	Linear range ($U\ mL^{-1}$)	LOD ($U\ mL^{-1}$)	Ref.
HRPzyme-*λ* exonuclease	CL	0.06 – 100	0.06	1
G-quadruplex/hemin DNAzyme	CL	0.01 – 0.8	0.01	2
localized TDN-PER	FL	8×10^{-5} – 0.1	1.8×10^{-5}	3
Padlock + LT + T4 PNK + T4 ligase	FL	10^{-3} – 0.1	3.8×10^{-4}	4
poly $(A)_n$-DITO-1	FL	0.1 – 10	0.02	5
3D DNA walking machine-DCR	FL	0.01 – 10	0.01	6
RCA-chemiluminescence	CL	0.01 – 3	2.2×10^{-4}	7
PeQDs-NCDs@HZIF-8/GCE	ECL	10^{-5}–0.05	6.2×10^{-6}	8
HP1/AuNP/g-C_3N_4/GCE	PEC	0.002 – 0.1	0.001	9
TiO_2/g-C_3N_4/CdS-CdSe-*λ*-Exo	PEC	10^{-4}–0.02	6.9×10^{-5}	10
DNAzyme-driven DNA walker	DPV	0.01 – 15	10^{-3}	11
AuNP-S2/MCH/S1/Au	DPV	10^{-3} – 10	7.76×10^{-4}	12
HRP-SA/S4/RCA/S1-TiO_2/Au	DPV	10^{-4} – 15	3×10^{-5}	13
zwitterionic peptide/Fe-MOF	DPV	10^{-3} – 10	5.5×10^{-4}	14
MB@PP5/TiO_2/P-DNA/Au	DPV	2×10^{-4} – 5	10^{-4}	15
Thi@PP5@MWCNTs/TiO_2/P-DNA/Au	**DPV**	**10^{-5} – 15**	**5×10^{-6}**	**This work**

References

1 C. Jiang, C. Y. Yan, J. H. Jiang and R. Q. Yu, *Anal. Chim. Acta*, 2013, **766**, 88–93.

2 H. S. Liu, C. B. Ma, J. Wang, H. C. Chen and K. M. Wang, *Anal. Biochem.*, 2017, **517**, 18–21.

3 Z. W. Xie, X. Y. Wang, S. Y. Chen, Z. X. Zhao, S. H. Zhao, W. X. Zhang, L. J. Luo and G. Yi, *Microchem. J.*, 2022, **183**, 107989.

4 Y. Cen, W. J. Deng, R. Q. Yu and X. Chu, *Talanta*, 2018, **180**, 271–276.

5 J. Zhu and L. T. Chen, *Anal. Chim. Acta*, 2022, **1221**, 340080.

6 Y. Q. Zhang, Q. Q. Cai, X. S. Yan and G. F. Jie, *Anal. Chim. Acta*, 2023, **1251**, 341003.

7 W. Tang, G. C. Zhu and C. Y. Zhang, *Chem. Commun.*, 2014, **50**, 4733–4735.

8 Y. Cao, Y. Zhou, Y. H. Lin and J. J. Zhu, *Anal. Chem.*, 2021, **93**, 1818−1825.

9 J. Y. Zhuang, W. Q. Lai, M. D. Xu, Q. Zhou and D. P. Tang, *ACS Appl. Mater. Interfaces*, 2015, **7**, 8330–8338.

10 P. P. Li, Y. Cao, C. J. Mao, B. K. Jin and J. J. Zhu, *Anal. Chem.*, 2019, **91**, 1563-1570.

11 J. X. Mao, X. Chen, H. H. Xu and X. Q. Xu, *J. Electroanal. Chem.*, 2020, **874**, 114470.

12 L. Cui, Y. Y. Li, M. F. Lu, B. Tang and C. Y. Zhang, *Biosens. Bioelectron.*, 2018, **99**, 1–7.

13 Y. L. Zhang, X. Fang, Z. Y. Zhu, Y. Q. Lai, C. L. Xu, P. F. Pang, H. B. Wang, C. Yang, C. J. Barrow and W. R. Yang, *RSC Adv.*, 2018, **8**, 38436–38444.

14 Z. Song, Y. Li, H. Teng, C. F. Ding, G. Y. Xu and X. L. Luo, *Sensor. Actuat. B-Chem.*, 2020, **305**, 127329.

15 D. Luo, Z. Q. Liu, A. W. Su, Y. L. Zhang, H. B. Wang, L. J. Yang, W. R. Yang and P. F. Pang, *Talanta*, 2024, **266**, 124956.